JCB

Supplemental material

Takao et al., https://doi.org/10.1083/jcb.201904156

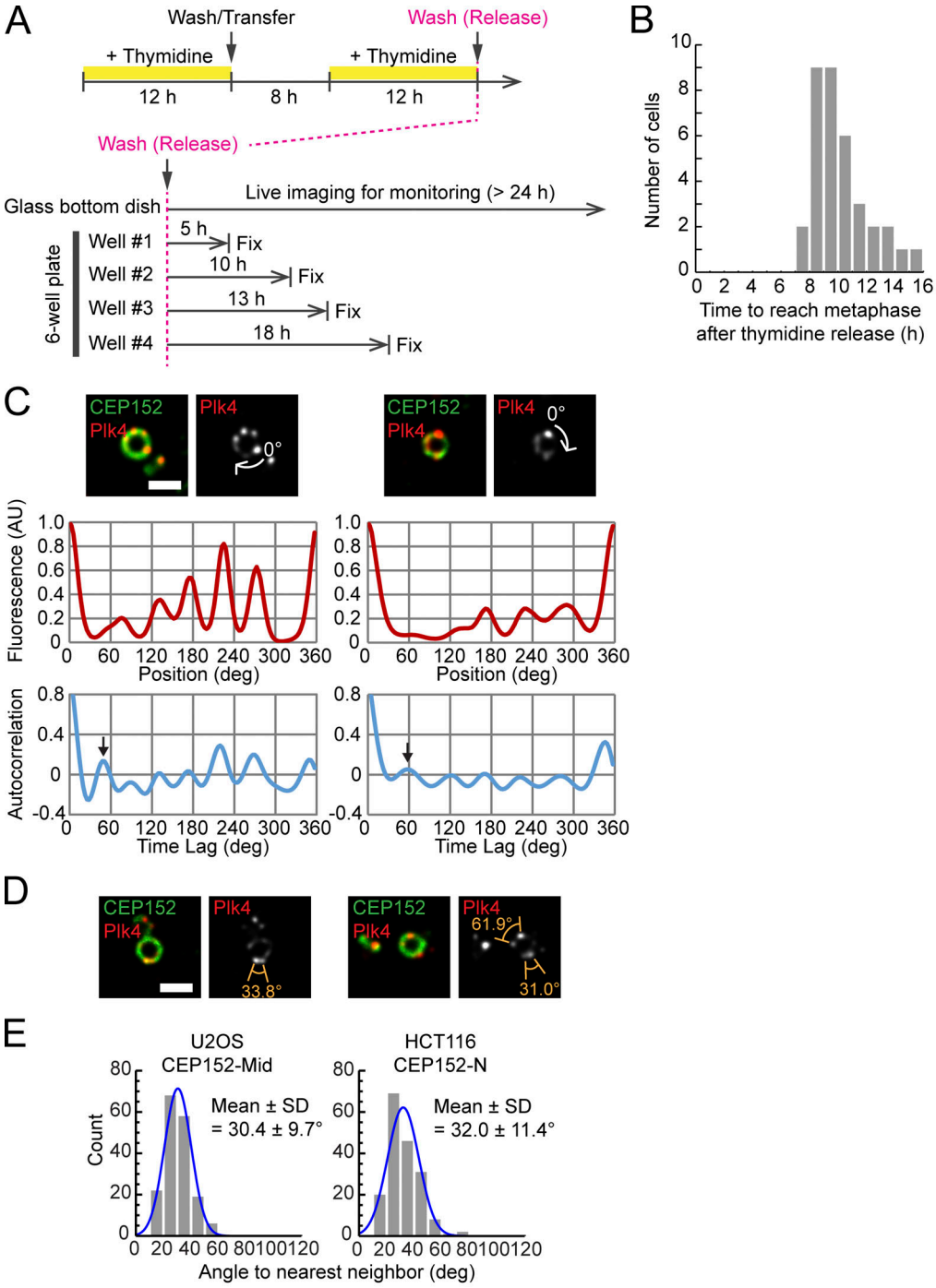

Figure S1. **Time course of cell synchronization and analyses for periodicity of spatial patterns of centriolar Plk4 and CEP152. (A)** Time course of sample preparation after the synchronization of cells. Cells were arrested twice with thymidine. Following the second thymidine release, cells were fixed for immunofluorescence at the indicated time points, while the cell cycle was monitored via live-cell imaging. **(B)** The time taken by the monitored live cells to reach metaphase after thymidine release. Most cells reached mitosis ∼9 h after thymidine release. **(C)** Examples of autocorrelation analysis. Representative STED images (top), oval profiles (middle), and autocorrelation functions (bottom) are shown. The arrows in the autocorrelation graphs indicate the primary peaks representing their periods. Scale bar, 0.5 µm. **(D)** Representative STED images of Plk4 with foci at ∼30° intervals. Although on average the discrete patterns of Plk4 exhibited a sixfold symmetry, neighboring Plk4 clusters occasionally localized with ∼30° intervals between peaks. This suggests that there may be 12 slots for Plk4 foci. Scale bar, 0.5 µm. **(E)** Extended analyses of the periodicity of CEP152. Results of measurements similar to those presented in Fig. 2 E but using a different antibody (left) or another cell line (right) are shown. Nearest-neighbor clustering analyses using an antibody recognizing another region of CEP152 (CEP152-Mid) or HCT116 cells confirmed the 30° periodicity or 12-fold rotational symmetry of the CEP152 patterns. However, it should be noted that the spatial patterns of CEP152 are somewhat less clear than the sharp, discrete patterns of Plk4 (Fig. 2). This could mean that the CEP152 scaffolds are more flexible and dynamic than we have supposed and that the 12-fold rotational symmetry we have observed is merely their average form. *n* = 19 and 20 cells, respectively.

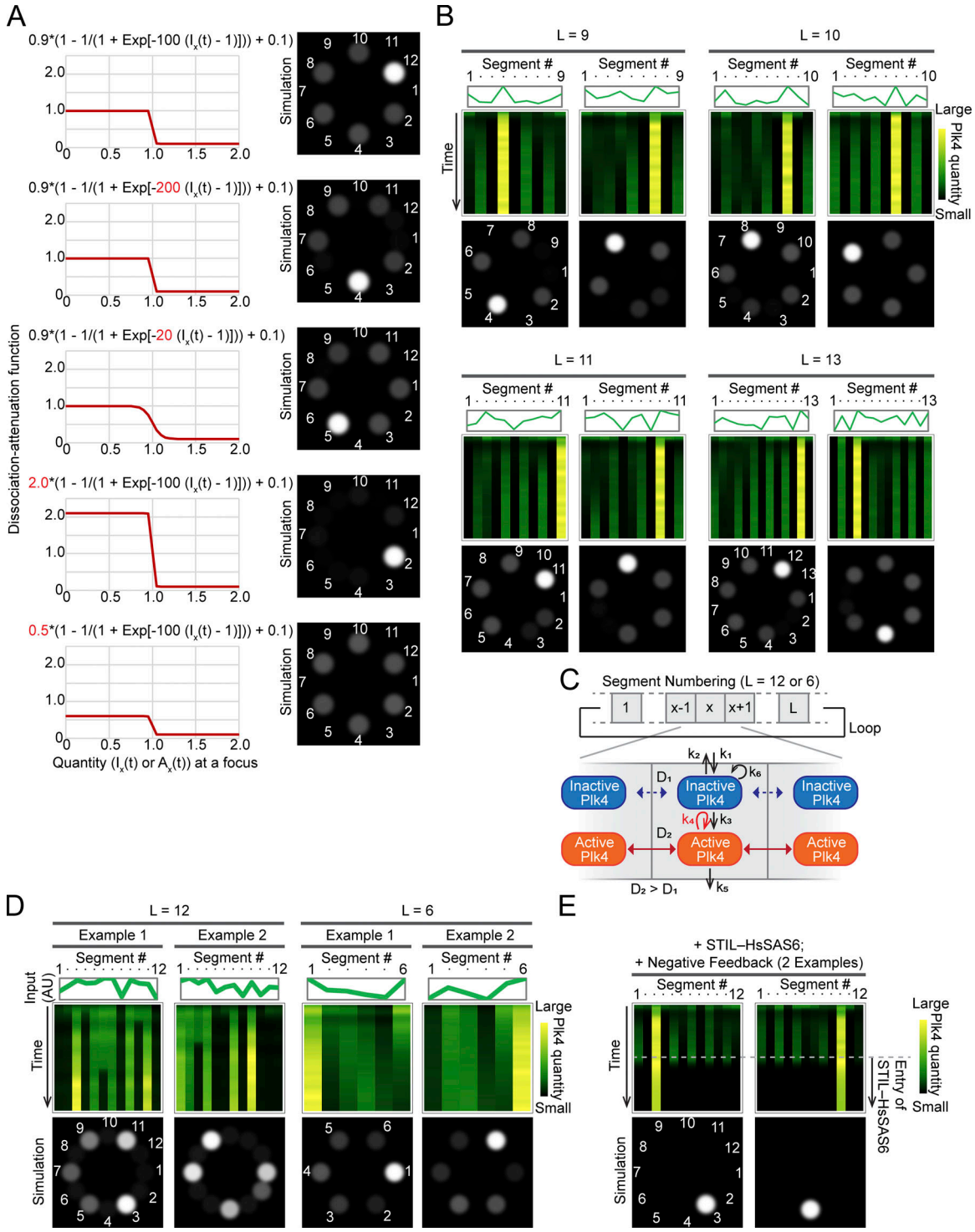

Figure S2. **Simulations with alternative parameter sets or assumptions. (A)** Representative plots of the dissociation-attenuation function and the dependency of the model on the function. The standard dissociation-attenuation function used in this study and a representative simulation result are shown in the top row. Results with a different parameter (red numbers in the function) are also shown for comparison. **(B)** Test of the dependency of the LI model on the number of Plk4 slots. The number of slots (L) was set to 9, 10, 11, or 13 (in addition to 12, as shown in Fig. 3, B and C). All simulations exhibited similar biased discrete patterns. Two examples are shown for each condition. **(C)** Schematic drawing of the RD model. **(D)** Example results of the simulations with the RD model. **(E)** Representative simulation results with the LI model using the assumption of negative-feedback regulation. In this additional assumption, the dissociation/degradation of Plk4 in the slots in the absence of STIL is promoted via negative-feedback regulation, mediated by the Plk4–STIL interaction. At the mid-point of the time course, the STIL–HsSAS6 complex began to accumulate. It stabilized the dominant focus of Plk4, as in Fig. 4 A, and affected the other segments negatively by promoting dissociation/degradation.

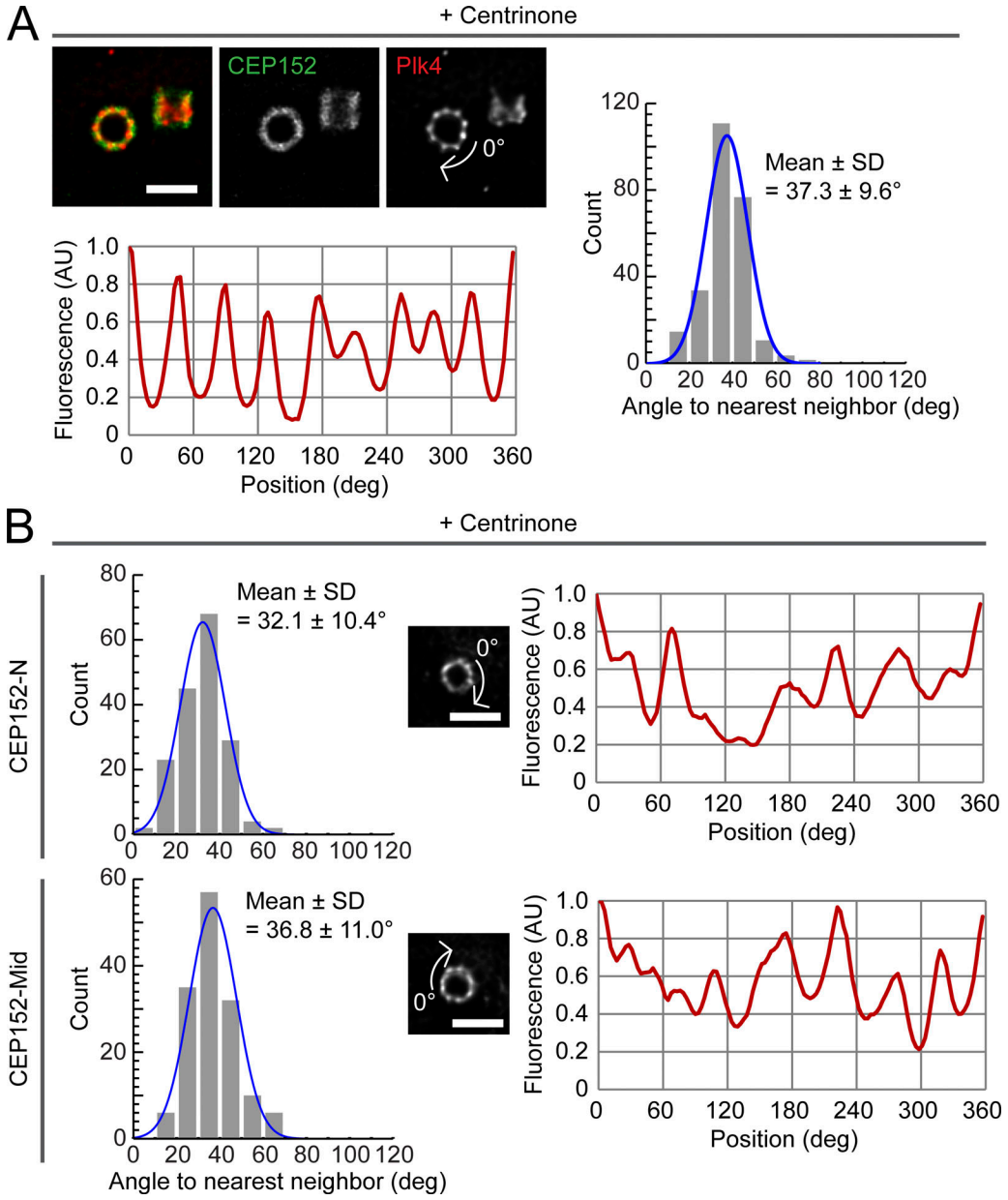

Figure S3. **The effect of the inhibition of kinase activity on the pattern formation of Plk4. (A)** STED pattern analysis of Plk4 in centrinone-treated cells. Data are displayed in a similar manner to those in Fig. 2. Scale bar, 0.5 µm. *n* = 30 cells. **(B)** STED pattern analysis of CEP152 in centrinone-treated cells. Results using two different antibodies (CEP152-N/Mid) are shown. The results suggest that the CEP152 scaffold may be more flexible and may also change its patterns around centrioles following treatment with centrinone, although it is important to consider that treatment with centrinone may also affect cytosolic Plk4. While centrinone is a powerful tool for the investigation of Plk4 functioning, alternative approaches may be necessary to precisely investigate the molecular dynamics in the nanoscopic space around centrioles. Scale bar, 0.5 µm. *n* = 29 and 18 cells, respectively.

Table S1. **Basic parameter settings for the LI model**

k_1	k_2	k_3	k_4	k_5	k_6	k_{max1}	k_{max2}	N	I_{cyto}
0.0001	0.01	0.008	0.01	0.1	0.04	0.02	0.06	(0.9, 1.1)	0.8

Table S2. **Basic parameter settings for the RD model**

k_1	k_2	k_3	k_4	k_5	k_6	k_{max1}	k_{max2}	N	I_{cyto}
0.0002	0.01	0.004	0.01	0.1	0.02	0.02	0.05	(0.9, 1.1)	1
D_I		D_A		dx					
10^{-6}		10^{-2}		0.01					